

Chien-Hsiung Tsai · Han-Taw Chen · Yao-Nan Wang
Che-Hsin Lin · Lung-Ming Fu

Capabilities and limitations of 2-dimensional and 3-dimensional numerical methods in modeling the fluid flow in sudden expansion microchannels

Received: 22 March 2006 / Accepted: 22 April 2006 / Published online: 8 June 2006
© Springer-Verlag 2006

Abstract This paper deals with computational and experimental investigations into pressure-driven flow in sudden expansion microfluidic channels. Improving the design and operation of microfluidic systems requires that the capabilities and limitations of 2-dimensional (2-D) and 3-dimensional (3-D) numerical methods in simulating the flow field in a sudden expansion microchannel be well understood. The present 2-D simulation results indicate that a flow separation vortex forms in the corner behind the sudden expansion microchannel when the Reynolds number is very low ($Re \sim 0.1$). However, the experimental results indicate that this prediction is valid only in the case of a sudden expansion microchannel with a high aspect ratio (aspect ratio $\gg 1$). 3-D computational fluid dynamics simulations are performed to predict the critical value of Re at which the flow separation vortex phenomenon is induced in sudden expansion microchannels of different aspect ratios. The experimental flow visualization results are found to be in good agreement with the 3-D numerical predictions. The present results provide designers with a

valuable guideline when choosing between 2-D or 3-D numerical simulations as a means of improving the design and operation of microfluidic devices.

Keywords Sudden expansion microchannel · Reynolds numbers · Flow separation vortex

1 Introduction

It is essential that the microchannels in microfluidic devices be carefully designed to meet the specific requirements of different applications (e.g., microfluidic mixing in microreaction chambers or injection and separation in capillary electrophoresis devices) and to control the interaction between the fluid and the channel wall in microfluidic fuel cells, microcoolers, etc. (Liu et al. 2005; Cohen et al. 2005; Lin et al. 2005; Tsai et al. 2005; Wang et al. 2006). Designing appropriate microchannel configurations is essential when developing microfluidic devices for biological or chemical analysis procedures as the characteristics of the microchannel determine the overall quality of the analytical results.

The large surface area-to-volume ratio of a microchannel induces a significant shear stress within the flow. Researchers have employed a variety of experimental and theoretical methods to analyze fluid flow in microchannels. Using numerical and experimental approaches, Tuckermann and Pease (1981) demonstrated that the friction coefficients for fluid flow through a microchannel were marginally higher than those predicted by classical theories for traditional large-scale channel flow. Urbanek et al. (1993) investigated liquid flow through order of $10 \mu\text{m}$ hydraulic diameter microchannels and also showed that the friction coefficients were somewhat higher than the classical predictions. Pfahler et al. (1990) reported that the measured friction coefficients in microchannel flow were independent of the Reynolds number (Re) at large values

C.-H. Tsai
Department of Vehicle Engineering, National Pingtung University of Science and Technology, Pingtung 912, Taiwan

H.-T. Chen · Y.-N. Wang
Department of Mechanical Engineering, National Cheng-Kung University, Tainan 701, Taiwan

C.-H. Lin (✉)
Department of Mechanical and Electro-Mechanical Engineering, National Sun Yat-sen University, Kaohsiung 804, Taiwan
E-mail: chehsin@mail.nsysu.edu.tw
Tel.: +886-7-5252000
Fax: +886-946-526044

L.-M. Fu (✉)
Graduate Institute of Materials Engineering, National Pingtung University of Science and Technology, Pingtung 912, Taiwan
E-mail: loudyfu@mail.npust.edu.tw
Tel.: +886-8-7703202
Fax: +886-8-7740552

of Re and demonstrated that the flow rate was higher than expected for both isopropanol and silicon oil. Peng and Peterson (1996) examined the forced-flow characteristics of water flow through microchannels with a wide range of hydraulic diameters. They observed that a laminar flow transition occurred at $Re = 200\text{--}700$ and showed that the value of Re at which the transition took place reduced with decreasing microchannel size. Fu et al. (2003) investigated the effect of a simple step change in zeta potential on electroosmotic flow in a rectangular microchannel. Their study indicated that an eruptive change of velocity profile occurs at the region of step change in zeta potential. However, no circulation in the flow field was observed in this study. In general, the experimental evidence indicates that microchannel flow is strongly dependent upon the type and properties of the working fluid and the geometric parameters of the microchannels.

The computational fluid dynamics (CFD) method is a highly convenient analytical instrument for microfluidic devices. The CFD method can successfully predict a range of fluid behaviors in microfluidic devices such as microfluidic fuel cells and rectifiers and can provide insights into electroosmotic flow or pressure-driven flow in microfluidic mixers, reactors, etc. (Bazylak et al. 2005; Burke and Regnier 2003; Vijayendran et al. 2003; Baroud et al. 2003; Sundaram and Tafti 2004; Coleman and Sinton 2005; Hardt et al. 2005). In modeling microchannel flows, 2-dimensional (2-D) and 3-dimensional (3-D) numerical simulation methods impose different assumptions. For example, 2-D simulations assume that the depth (i.e., the z -direction) of the microchannel geometry is infinite or that the flow takes place at a low Reynolds number. However, in many cases, the commonly used 2-D (Jen and Lin 2002; Tomomura et al. 2004; Sundaram and Tafti 2004; Pan et al. 2004; Croce and D'Agro 2004, 2005; Townsend et al. 2005) or 3-D (Koo and Kleinstreuer 2003; Tripathi et al. 2005; Rawool et al. 2006; Rawool and Mitra 2006) numerical methods successfully provide accurate predictions of the flow behavior inside microchannels. In general, the success of using 2-D numerical methods depends upon the characteristics of the flow, e.g., the Reynolds number, Strouhal number, etc. Therefore, it is necessary to establish the critical values of these physical characteristics at which 2-D simulations are no longer applicable and must be replaced by 3-D numerical methods.

Sudden expansion microchannels are commonly applied in fuel cell devices (Liu et al. 2005; Lin et al. 2005) or biochips (Walker et al. 2005; Hibara et al. 2005). The performance of such devices is influenced by the onset of flow separation. It is generally accepted that the flow separation vortices are induced in microchannels of this type when the Reynolds number of the flow exceeds a certain critical value, but a systematical investigation into this characteristic of sudden expansion microchannel is still lacking. This study performs 2-D and 3-D numerical simulations to investigate fluid flow behavior

in a sudden expansion microchannel. The numerical results are then compared to the experimental findings. The aims of this study are: (1) to identify the critical value of the Reynolds number at which flow separation occurs in sudden expansion microchannels of different aspect ratios and (2) to investigate the limitations and capabilities of 2-D and 3-D numerical methods in modeling the fluid flow. Figure 1 presents an optical microscope image of the sudden expansion microchannel under current consideration and a scanning electron microscope image of its cross-section. The grid applied in the current numerical simulations is also shown.

2 Experimental section

2.1 Chip fabrication

The sudden expansion microchannels were fabricated on glass microscope slides ($76 \times 26 \times 1 \text{ mm}^3$, Marienfeld, Germany) using the rapid, low-cost method presented previously by the current authors in (Fu et al. 2002; Lin et al. 2004). To reduce the complexity and expense of the fabrication process, a $3\text{-}\mu\text{m}$ -thick AZ 4620 (Clariant, Somerville, NJ, USA) positive photoresist layer was used in place of a metal layer as an etching mask to define the required microfluidic structures. The microchannels were formed using a modified buffered oxide glass etching technique with an etching rate of $0.9 \mu\text{m}/\text{min}$. The average surface roughness (R_a) of the etched surface was carefully controlled to be less than 20 \AA ($7 \times 7 \mu\text{m}^2$ AFM scan area, see Fig. 1c). The etched

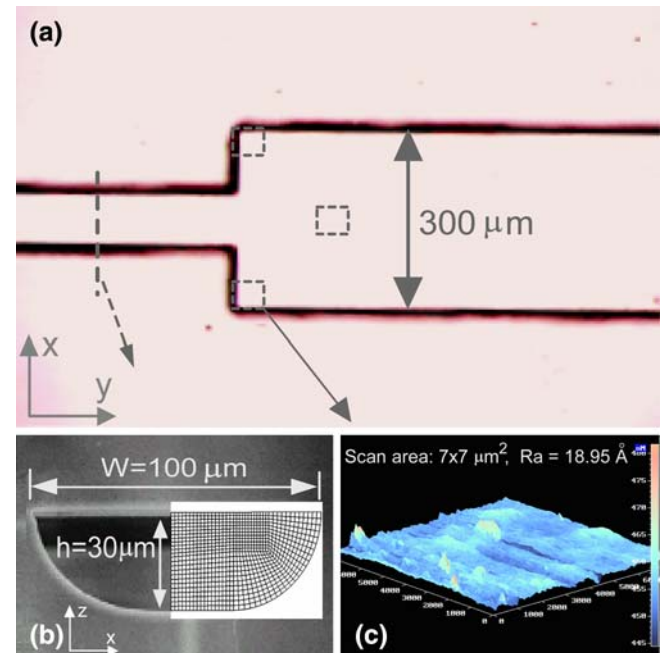


Fig. 1 a Optical microscope image of sudden expansion microchannel. b Scanning electron microscope image and numerical grid of microchannel cross-section. c AFM image of the etched surface

substrates were then thermally bonded with drilled upper substrates in a sintering oven at a temperature of 580°C for 10 min to form the sealed sudden expansion microchannels. Finally, a Teflon tube of 500- μm inner diameter and 1.5-mm outer diameter was attached to the fluid-inlet hole on the upper substrate using epoxy glue.

2.2 Experimental setup

Figure 2 shows the schematic presentation of the experimental setup for this study. The experiments were performed under a lab-built PIV (particle image velocimeter) system composed of a 100-W fluorescent microscope (Model E400 Nikon, Kanagawa, Japan) for fluorescence excitation and a shutter controllable CCD (Model DXC-190, Sony, Tokyo, Japan) camera for capturing the experimental images. The image-capturing rate was 30 fps with the resolution of 640×480 pixels. In order to get better experimental images using the PIV system, sample fluid of DI water doped with three different-diameter green fluorescent microspheres (1-, 2- and 5- μm diameter, Duke Scientific Corp., Palo Alto, CA, USA) was used in this study. In general, bigger particles will emit higher fluorescence intensity under fluorescent excitation and will result in a clearer and better image quality. However, the inertia of big particles is much larger than small particles so that it was difficult for big particles to flow into the separation vortex but not for the small particles. The 2- μm particles were used to smoothen the image contrast between the 1- and 5- μm particles. The mixing ratio of these three microspheres was 1:1:1 and the particle doping concentration for the sample fluid was around 1% (volume percent). The sample fluid was driven into the microchip device using a programmable syringe pump (200 series, KD Scientific, Holliston, MA, USA) via the Teflon tubing. The experimental images acquired by the CCD were recorded via a high-speed image acquisition interface (DVD PKB, V-gear, Taiwan).

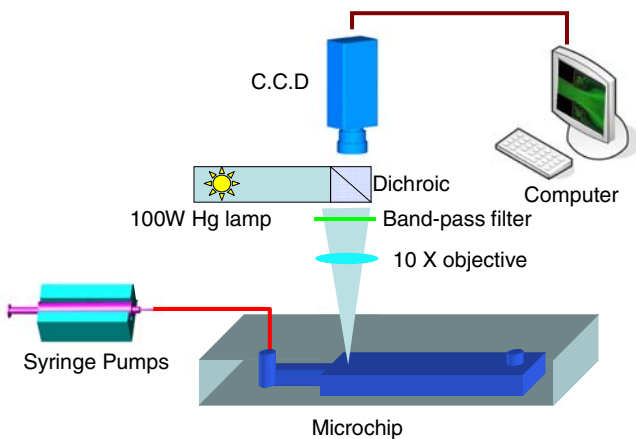


Fig. 2 Schematic of experimental setup

3 Computational simulations

In general, comprehensive CFD simulations are conducted before physical models are built and tested because these simulations enable all of the parameters to be varied over a wide range of values and permit simultaneous and instantaneous data collection throughout the model. Performing numerical simulations is an important step in optimizing microchannel designs and enables the experimental results to be reliably interpreted.

The flow field of a sudden expansion microchannel is governed by the incompressible Navier–Stokes equations. The governing mass and momentum equations can be written as follows:

$$\nabla_i u_i = 0, \quad (1)$$

$$\rho \frac{\partial u_i}{\partial t} + \rho (u_j \times \nabla_j) u_i = -\nabla_i p + \mu \nabla^2 u_i, \quad (2)$$

where u_i denotes the fluid velocity, ρ the density, μ the viscosity and p the pressure. In the present simulations of the flow of doped DI water, ρ and μ are specified as 1,000 kg/m³ and 0.001 kg/m/s, respectively.

As recommended by Hardt et al., the present governing equations are cast into a set of finite difference equations using the third-order QUICK scheme in order to minimize numerical diffusion (Hardt and Schonfeld 2003). The technique employed here is the finite volume method. The SIMPLEX algorithm (Van Doormal and Raithby 1984) is then used to solve the resulting difference equations.

In the present simulations, the inlet velocity is specified in the range 0.12–60 cm/s, corresponding to $Re = 0.1$ –50. Note that Re is defined as:

$$Re = \frac{\rho u D_h}{\mu},$$

where D_h is the hydraulic diameter of the inlet microchannel. The simulations assume fully developed flow conditions in the outlet microchannel and impose a no-slip boundary condition at the microchannel wall.

In order to ensure a good resolution of the numerical results, the computational domain is discretized using a hexahedral mesh in which most of the cells have sides of length 2 μm . The computational domain contains approximately 800,000 cells.

4 Results and discussions

Initially, a 2-D simulation was performed of the flow field in a microchannel with an expansion ratio of 3 (outlet width/inlet width = 300 μm /100 μm) and Re values of 0.1 and 30. As shown in Fig. 3a, the 2-D numerical results predict the formation of a flow separation vortex in the corner behind the sudden expansion microchannel at very low Reynolds numbers ($Re \sim 0.1$).

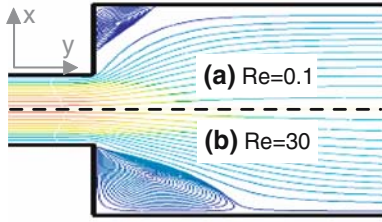


Fig. 3 Two-dimensional numerical simulation results for streamline distributions in sudden expansion microchannel with expansion ratio of 3 at different Re : **a** $Re = 0.1$, and **b** $Re = 30$

The results show that this vortex expands as the value of Re increases (Fig. 3b). In all the simulations at Re values of 0.1–0.01, the separation vortex still occurred in this corner with the same shape as shown in Fig. 3a. Several numerical experiments have been conducted to find that the 2-D method fails to predict the critical Reynolds number over which the separation vortex is formed.

In order to better understand the flow structure in the sudden expansion microchannel, 3-D numerical simulations were performed to investigate the flow field for various expansion ratios, entry region aspect ratios and Reynolds numbers. Figure 4 presents the 3-D streamlines of the steady-state flow field in a microchannel with an expansion ratio of 3 (outlet width/inlet width = 300 μm /100 μm), an entry region aspect ratio of 1/2 (depth/width = 50 μm /100 μm) and Re values of 10, 30 and 50. The critical value of Re , i.e., the value of Re at which flow separation is induced in the sudden expansion microchannel, is found to be 22.5. It can be seen that when Re is lower than this value, flow separation does not occur and the streamlines flow smoothly from the inlet to the outlet. However, as shown in Fig. 4b, when Re is higher than this critical value, a flow separation vortex is induced in the inner region of the sudden expansion microchannel. Figure 4c shows that this separation vortex expands to fill virtually the entire expansion corner when the Reynolds number increases to $Re = 50$. Comparing Fig. 4 with Fig. 3, it can be seen that the flow separation vortex predicted by the 3-D numerical simulation method occurs at a higher value of Re than that indicated by the 2-D numerical results.

For three different values of Re , Fig. 5 compares the streamline distributions observed experimentally with those predicted by the 3-D numerical simulation method at a cross-section located at a depth of 20 μm in a sud-

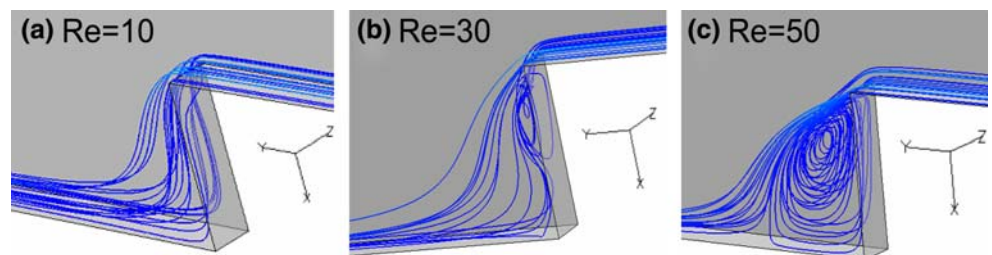
den expansion microchannel with an expansion ratio of 3 and an aspect ratio of 1/2. It is observed that a good qualitative agreement exists between the experimental results and the numerical predictions in every case. Figure 6a plots the experimental and numerical results for the critical value of Re for the case of sudden expansion microchannels with a constant expansion ratio of 3 but different aspect ratios. When Re lies above the curve, a flow separation vortex is formed in the sudden expansion microchannel. Conversely, when Re lies below this curve, flow separation does not take place. Figure 6a also plots the results obtained from the 3-D numerical simulation method for sudden expansion microchannels with rectangular cross-sections (x - z section). It is observed that the sudden expansion microchannels of two different cross-section geometries have virtually identical critical values of Re . The critical Re decreases with the increase of aspect ratio. The critical Re approaches zero asymptotically as the aspect ratio becomes infinite. The zero critical Re concurred with the results predicted by 2-D numerical method. Figure 6b plots the critical Re curve for sudden expansion microchannels with a constant aspect ratio of 1/2 (50 μm deep) but different expansion ratios. It can be seen that the critical value of Re is insensitive to the expansion ratio.

Figure 7 presents the 3-D streamlines of the steady-state flow field in a sudden expansion microchannel with an expansion ratio of 3 (outlet width/inlet width = 300 μm /100 μm), an entry region aspect ratio of 1 (depth/width = 100 μm /100 μm) and Re values of 5 and 30. For this particular aspect ratio, the flow separation vortex is induced in the outer region of the microchannel (see Fig. 7a). The region at which the separation vortex stayed in the early stage is different from that observed in the microchannel with lower aspect ratio as shown in Fig. 5c, d. For all the simulations in this study, the vortex formed in the inner convex corner if aspect ratio ≤ 0.5 ; but it formed in the outer concave corner as aspect ratio ≥ 1 .

5 Conclusions

This study has analyzed 2-D and 3-D numerical simulation predictions for fluid flow behavior in sudden expansion microchannels. The 2-D simulation results have shown the formation of a flow separation vortex in

Fig. 4 Three-dimensional numerical simulation results for streamline distributions in sudden expansion microchannel with expansion ratio of 3 and aspect ratio of 1/2 at different Re : **a** $Re = 10$, **b** $Re = 30$ and **c** $Re = 50$



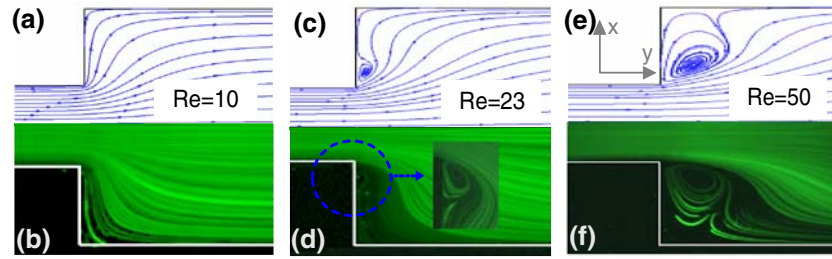


Fig. 5 Comparison of experimental and numerical streamline distribution in sudden expansion microchannel with expansion ratio of 3 and aspect ratio of 1/2 at different Re : **a** $Re = 10$ (numerical), **b** $Re = 10$ (experimental), **c** $Re = 23$ (numerical), **d** $Re = 23$ (experimental), **e** $Re = 50$ (numerical) and **f** $Re = 50$ (experimental)

Fig. 6 **a** Numerical and experimental evaluations of critical Re in sudden expansion microchannel with expansion ratio of 3 and different aspect ratios. **b** Numerical and experimental evaluations of critical Re in sudden expansion microchannel with aspect ratio of 1/2 and different expansion ratios

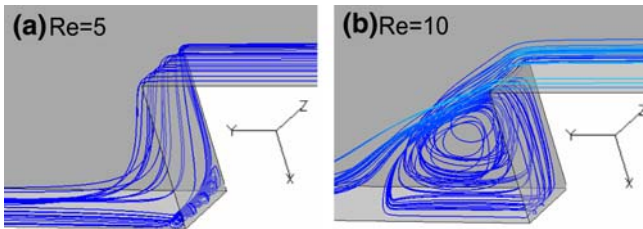
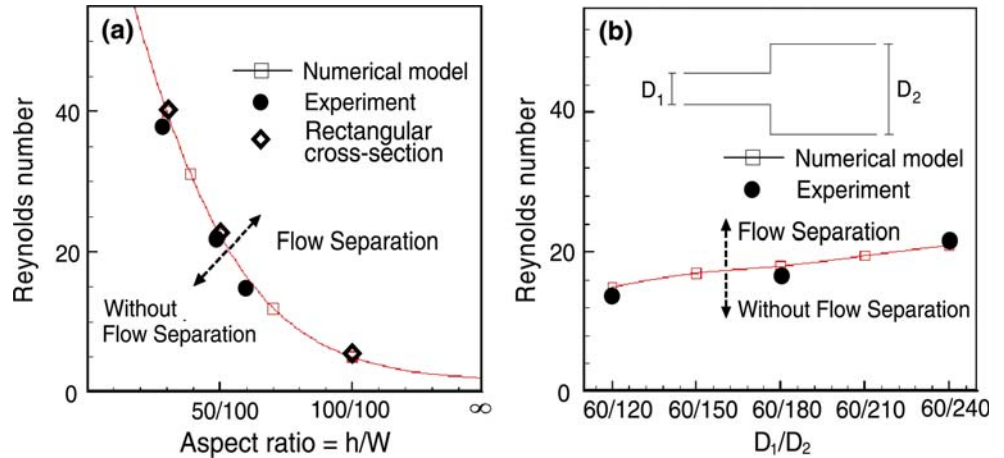


Fig. 7 Three-dimensional numerical simulation results for streamline distributions in sudden expansion microchannel with expansion ratio of 3 and aspect ratio of 1 at different Re : **a** $Re = 5$ and **b** $Re = 10$

the corner behind the sudden expansion microchannel at very low Reynolds numbers. This result is only consistent with the 3-D numerical results when the aspect ratio of the sudden expansion microchannel is very high (i.e., $\gg 1$). Hence, it is recommended that the 2-D simulation method only be applied to predict the flow behavior in sudden expansion microchannels with high aspect ratios. The 3-D simulation results have indicated that when Re exceeds a certain critical value (strongly dependent on the aspect ratio of the microchannel), a flow separation vortex is induced. The predictions of the 3-D numerical simulations are consistent with the experimental observations. For the onset of separation vortex, the vortex is formed in the inner convex corner if aspect ratio ≤ 0.5 ; but in the outer concave corner as

aspect ratio ≥ 1 . The results presented in this study are of value to designers considering the use of either 2-D or 3-D numerical simulations to improve the design and operation of microfluidic devices containing sudden expansion microchannels such as microfluidic fuel cells or biochips.

Acknowledgments The authors gratefully acknowledge the financial support provided to this study by the National Science Council, Taiwan, under Grant Nos. NSC-94-2320-B-020-001 and NSC-94-2320-B-110-003. The authors would like to thank NPUST ME Microchip Fabrication Center for access of equipments.

References

- Baroud CN, Okkels F, Menetrier L, Tabeling P (2003) Reaction-diffusion dynamics: confrontation between theory and experiment in a microfluidic reactor. *Phys Rev E* 67:60104
- Bazylak A, Sinton D, Djilali N (2005) Improved fuel utilization in microfluidic fuelcells: a computational study. *J Power Sources* 143:57–66
- Burke BJ, Regnier FE (2003) Stopped-flow enzyme assays on a chip using a microfabricated mixer. *Anal Chem* 75:1786–1791
- Cohen JL, Westly DA, Pechenik A, Abruna HD (2005) Fabrication and preliminary testing of a planar membraneless microchannel fuel cell. *J Power Sources* 139:96–105
- Coleman TT, Sinton AD (2005) A sequential injection microfluidic mixing strategy. *Microfluidics Nanofluidics* 1:319–327
- Croce G, D'Agro P (2004) Numerical analysis of roughness effect on microtube heat transfer. *Superlattices Microstruct* 35:601–616

- Croce G, D'Agro P (2005) Numerical simulation of roughness effect on microchannel heat transfer and pressure drop in laminar flow. *J Phy D* 38:1518–1530
- Fu LM, Yang RJ, Lee GB, Liu HH (2002) Electrokinetic injection techniques in microfluidic chips. *Anal Chem* 74:5084–5091
- Fu LM, Lin JY, Yang RJ (2003) Analysis of electroosmotic flow with step change in zeta potential. *J Colloid Interface Sci* 258:266–275
- Hardt S, Schönfeld F (2003) Laminar mixing in different interdigital micromixers: II. Numerical simulations. *AIChE J* 49:578–584
- Hardt S, Drese AKS, Hessel AV, Schönfeld F (2005) Passive micromixers for applications in the microreactor and μ TAS fields. *Microfluidics Nanofluidics* 1:108–118
- Hibara A, Iwayama S, Matsuoka S, Ueno M, Kikutani Y, Tokeshi M, Kitamori T (2005) Surface modification method of microchannels for gas–liquid two-phase flow in microchips. *Anal Chem* 77:943–947
- Jen CP, Lin YC (2002) Design and simulation of bi-directional microfluid driving systems. *J Micromech Microeng* 12:115–121
- Koo J, Kleinstreuer C (2003) Liquid flow in microchannels: experimental observations and computational analyses of microfluidics effects. *J Micromech Microeng* 13:568–579
- Lin CH, Fu LM, Chien YS (2004) Microfluidic T-form mixer utilizing switching electroosmotic flow. *Anal Chem* 76:5265–5272
- Lin CH, Tsai CH, Fu LM (2005) A rapid 3-dimensional vortex micromixer utilizing self-rotation effect under low Reynolds number conditions. *J Micromech Microeng* 15:935–943
- Liu S, Pu Q, Gao L, Korzeniewski C, Matzke C (2005) From nanochannel-induced proton conduction enhancement to a nanochannel-based fuel cell. *Nano Lett* 5:1389–1393
- Pan CT, Chuang HS, Cheng CY, Yang CT (2004) Micro-flow measurement with a laser diode micro-particle image velocimetry. *Sens Actuators A* 116:51–58
- Peng XF, Peterson GP (1996) Convective heat transfer and flow friction for water flow in microchannel structures. *Int J Heat Mass Transf* 39:2599–2608
- Pfahler J, Harley J, Bau HH, Zemel J (1990) Liquid transport in micron and submicron channels. *Sens Actuators A* 22:431–437
- Rawool AS, Mitra SK (2006) Numerical simulation of electroosmotic effect in serpentine channels. *Microfluidics Nanofluidics* 2:261–269
- Rawool AS, Mitra SK, Kandlikar SG (2006) Numerical simulation of flow through microchannels with designed roughness. *Microfluidics Nanofluidics* 2:215–221
- Sundaram N, Tafti DK (2004) Evaluation of microchamber geometries and surface conditions for electrokinetic driven mixing. *Anal Chem* 76:3785–3793
- Tomomura O, Tanaka S, Noda M, Kano M, Hasebe S, Hashimoto I (2004) CFD-based optimal design of manifold in plate-fin microdevices. *Chem Eng J* 101:397–402
- Townsend RJ, Hill M, Harris NR, White NM, Beeby SP, Wood RJK (2005) Fluid modelling of microfluidic separator channels. *Sens Actuators B* 111–112:455–462
- Tripathi A, Bozkurt O, Chauhan A (2005) Dispersion in microchannels with temporal temperature variations. *Phys Fluids* 17:103607
- Tsai CH, Tai CH, Fu LM, Wu FB (2005) Experimental and numerical analysis of the geometry effects of low-dispersion turns in microfluidic systems. *J Micromech Microeng* 15:377–385
- Tuckermann DB, Pease RFW (1981) High-performance heat sinking for VLSI. *IEEE Electron Device Lett* 2:126–129
- Urbanek W, Zemel JN, Bau HH (1993) An investigation of the temperature dependence of Poiseuille numbers in microchannel flow. *J Micromech Microeng* 3:206–209
- Van Doormal JP, Raithby GD (1984) Enhancements of the SIMPLE method for predicting incompressible fluid flows. *Numerical Heat Transf* 7:147–163
- Vijjayendran RA, Motsegood KM, Beebe DJ, Leckband DE (2003) Evaluation of a three-dimensional micromixer in a surface-based biosensor. *Langmuir* 19:1824–1828
- Walker GM, Sai JQ, Richmond A, Stremmer M, Chung CY, Wikswo JP (2005) Effects of flow and diffusion on chemotaxis studies in a microfabricated gradient generator. *Lab Chip* 5:611–618
- Wang K, Yue S, Wang L, Jin A, Gu C, Wang P, Feng Y, Wang Y, Niu H (2006) Manipulating DNA molecules in nanofluidic channels. *Microfluidics Nanofluidics* 2:85–88